Commissioning of electron cooling in CSRe

CPC(HEP & NP), 2010, **34**(7): 998–1004 **Chinese Physics C** Vol. 34, No. 7, Jul., 2010

Commissioning of electron cooling in CSRe*

YANG Xiao-Dong(杨晓东)[1;1)] MAO Li-Jun(冒立军)[1] LI Guo-Hong(李国宏)[1]
LI Jie(李杰)[1] MA Xiao-Ming(马晓明)[1] YAN Tai-Lai(晏太来)[1]
YUAN You-Jin(原有进)[1] SONG Ming-Tao(宋明涛)[1] YANG Jian-Cheng(杨建成)[1]
LIU Yong(刘勇)[1] ZHAO Tie-Cheng(赵铁成)[1] XIA Jia-Wen(夏佳文)[1]
ZHANG Wei(张玮)[1] GAO Da-Qing(高大庆)[1] ZHOU Zhong-Zu(周忠祖)[1]
YAN Hong-Bin(燕宏斌)[1] MAO Rui-Shi(毛瑞士)[1] HE Yuan(何源)[1]
HAN Shao-Fei(韩少斐)[1] ZHENG Jian-Hua(郑建华)[1] YANG Xiao-Tian(杨晓天)[1]
ZHAO Hong-Wei(赵红卫)[1] XIAO Guo-Qing(肖国青)[1] YIN Da-Yu(殷达钰)[1]
LI Peng(李朋)[1] JIA Huan(贾欢)[1] Parkhomchuk Vasily[2]
Reva Vladimir[2] Skorobogatov Dmitry[2]

[1] Institute of Modern Physics, CAS, Lanzhou 730000, China
[2] Budker Institute of Nuclear Physics, Novosibirsk, RAS 630090, Russia

Abstract The 400 MeV/u $^{12}C^{6+}$ ion beam was successfully cooled by the intensive electron beam near 1 A in CSRe. The momentum cooling time was estimated near 15 s. The cooling force was measured in the cases of different electron beam profiles, and the different angles between the ion beam and electron beam. The lifetime of the ion beam in CSRe was over 80 h. The dispersion in the cooling section was confirmed as positive close to zero. The beam sizes before cooling and after cooling were measured by the moving screen. The beam diameter after cooling was about 1 mm. The bunch length was measured with the help of the signals from the beam position monitor. The diffusion was studied in the absence of the electron beam.

Key words CSRe, electron cooling, hollow electron beam

PACS 29.20.db, 41.85.Ew, 29.20.dk

1 Introduction

HIRFL-CSR [1] is a new ion cooler-storage-ring system in IMP China. It consists of a main ring (CSRm) and an experimental ring (CSRe). The two existing cyclotrons SFC (K=69) and SSC (K=450) of the Heavy Ion Research Facility in Lanzhou (HIRFL) are used as its injector system. The heavy ion beams from HIRFL are injected into CSRm, then accumulated, e-cooled and accelerated, before being extracted to CSRe for internal-target experiments and other physics experiments.

CSRe is a 128.8 m circumference cooler storage ring with sixteen 22.5 degree C-type bending dipole magnets. The maximum β functions are 30.9 m and 22.3 m in the horizontal and vertical planes respectively. The maximum dispersion is 7.8 m, the dispersion at the injection point is zero, and the β function is 30.4 m in the Septum. The β functions at the electron cooler are 12.5 m and 16 m in the two transverse directions respectively, and the dispersion is near zero here. The tunes are about 2.53 and 2.57, the transition gamma is 2.629, and the transverse acceptance of CSRe is about 150 πmmmrad, and the longitudinal one is $\pm 5\times10^{-3}$.

The accelerated ion beam from the CSRm through the radioactive beam separator line with the length of 100 m is injected into the CSRe. Generally the CSRe is operated with the DC mode. A gas jet internal target is installed on the opposite side of the electron cooler.

The electron cooling device plays an important

Received 21 August 2009
* Supported by NSFC(10975166, 10905083, 10921504)
1) E-mail: yangxd@impcas.ac.cn

role in the HIRFL-CSR experimental ring for the heavy ion beam. Continuous electron cooling is applied to the stored ion beam for the compensation of the heating by various scattering. The most important thing is the ability to cool the ion beams to the highest quality for physics experiments with stored highly charged ions. The new state-of-the-art electron cooling device was designed and manufactured in the collaboration between BINP and IMP. It has three distinctive characteristics, namely high magnetic field parallelism in the cooling section, variable electron beam profile and electrostatic bending in toroids. The main parameters are listed in Table 1. The electron cooling devices of HIRFL-CSR were reported in many conferences [2–6]. The previous commissioning results have been given in the COOL05-P02 [7] and COOL07-TUM1I02 [8].

Table 1. Parameters of the CSRe electron cooler.

parameter	value
maximum electron energy	300 keV
maximum electron current	3 A
gun perveance	29 μP
cathode diameter	29 mm
current collection efficiency	$\geqslant$99.99%
maximum magnetic field in gun section	0.5 T
maximum magnetic field in cooling section	0.15 T
field parallelism in cooling section	4×10^{-5}
effective length of cooling section	3.4 m
vacuum pressure	$\leqslant 3\times10^{-11}$ mb

2 Beam cooling experiments

2.1 Beam position monitor

The basic principle of electron cooling requires that the ion beam should be parallel with the electron beam. In this case, two sets of capacitive cylinder beam position monitors were installed at the ends of the electron cooling section. The electron beam was modulated by an external 3 MHz signal. The signals picked up by four probes were magnified by four independent preamplifiers. The NI-5105 (8-channel High-Density Digitizer) was employed as main data acquisition and the data were processed by the special code of LabView.

The ion beam became bunched one after RF capture, the ion beam position was measured at this moment.

From these results, the angles and displacements between ion and electron beams in the horizontal and vertical planes were derived. According to the information, the closed-orbit of ion beam in the ring was corrected, the ion beam positions at the ends of cooling section were close to parallel with the electron beam, the electron beam was slightly adjusted with the help of correction coils of cooler in the cooling section, the ion beam and electron beam were matched well finally and the cooling was observed. A small displacement between two beams was not critical due to the bigger size of the electron beam.

2.2 Beam cooling results

Because the electron cooler is located near the injection point and just before the injection kicker, the injection efficiency and the closed-orbit correction should be compromised. In this case, four additional correction coils in the dipoles before and after the electron cooler operated at ramping mode. In the injection interval, these coils were ramped to the proper value, and then returned to the normal value to keep the correct orbit in the cooling section. During the commission, the electron beam was set as plat profile.

At the beginning, 200 MeV/u $^{12}C^{6+}$ was injected into CSRe, the magnetic field of electron cooler was set as a quarter of the maximum value. In this case, the magnetic field in the cooling section was 0.0385 T, and the electron beam current was set as 300 mA. After the orbit correction and regulation of the electron beam angle, the cooling was observed, but the cooling process was not fast enough. It could be caused by the poor quality of the high energy electron beam confined by a weak magnetic field in toroid, where additional transverse temperature was introduced. For a lack of proper transverse beam profile monitor, the moving screen was employed as a scrapper to measure the profile of the cooled ion beam. After the screen was moved near the centre of ion beam, the DC current transformer (DCCT) signal of the ion beam could not be recognized from the noise, but the Schottky signal was clear for observing the ion beam. The momentum spread in the range of 10^{-6} was observed in the case of low ion intensity.

At a given value of the stored particle number, the momentum spread is determined by the equilibrium between the electron cooling and various heating effects, the main one is an intrabeam scattering (IBS). At large intensity the momentum spread $\Delta P/P$ is scaled with the stored particle number N in accordance with a power law $\Delta P/P \propto N^{\kappa}$, where the power coefficient κ depends on the settings of the storage ring and the cooling system [9], and the value is determined by the misalignment angle between the ion beam and the electron beam during the cooling [10].

The measured minimum momentum spread at low intensity is determined by the stability of the magnetic field of the ring dipole and the electron beam energy, it is also limited by the detection technique.

The longitudinal signal of the ion beam was recorded by the spectrum analyzer for 200 s after one injection. Schottky signal in the electron cooling process is illustrated in Fig. 1, the momentum spread calculated from the data file. The momentum spread varying as the time in cooling is shown in Fig. 2, finally the momentum spread keeps constant. The Schottky signal distribution before and after the electron cooling is shown in Fig. 3.

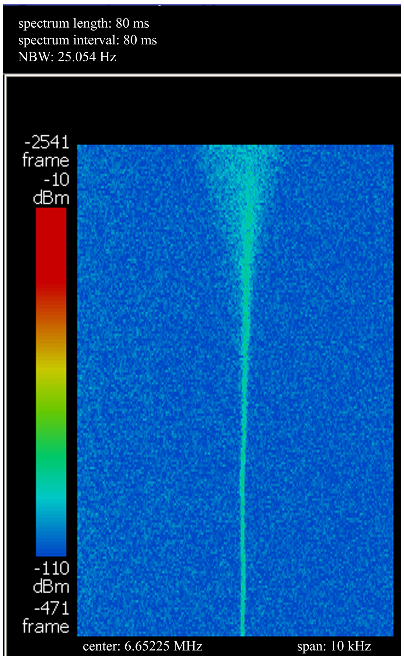

Fig. 1. Schottky signal of electron cooling process, the longitudinal signal was recorded by the spectrum analyzer for 200 s after one injection.

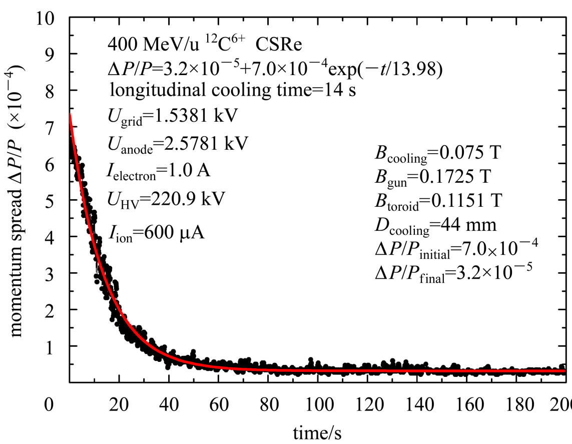

Fig. 2. The momentum spread as a function of time during cooling.

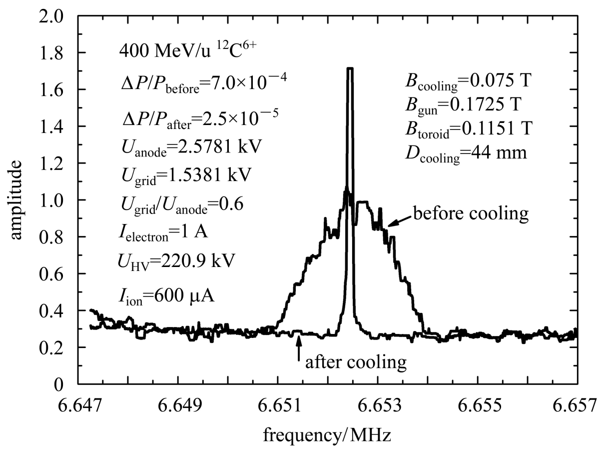

Fig. 3. The momentum spread before and after cooling.

2.3 Longitudinal cooling force measurement

The electron energy-step method [11] is one of the straightforward techniques for measuring the longitudinal cooling force. The ion beam has been cooled first the ion and electron velocities were matched well. The electron energy was jumped rapidly by changing the cathode potential, a well defined velocity difference between the ions and the electrons was created. The ions will be accelerated or decelerated toward the new electron velocity. The acceleration is determined via Schottky signal from the change in revolution frequency per unit time.

The Tektronix RSA3303A real-time spectrum analyzer was used in experiments. The 4^{th} harmonic centre frequency shift was calculated using the spectra files recorded by the analyzer. This method was applicable to relative velocities from 10^3 to 10^6 m/sec. The behaviour of a cooled $^{12}C^{6+}$ beam after applying a step of 410 eV is illustrated in Fig. 4 [12].

After the ion beam was cooled down, a sudden jump of electron beam energy created a difference between the energies of ion and electron, due to the cooling, the ions were dragged to the new matching energy, and new equilibrium was established again. From the momentum variety, and the time interval, with the help of formula $F\cdot\Delta t=\Delta P$, the longitudinal cooling force was derived.

The experiments were performed using the electron energy-step method described above. The experimental conditions are summarized as Table 2. These standard operational parameters were determined by HIRFL-CSRe optimization. The profile of electron beam was controlled by the ratio between the potentials of grid and anode.

Table 2. The parameters of electron cooler in experiments.

ion energy/(MeV/u)	B_{gun}/T	B_{toroid}/T	$B_{cooling\ section}$/T	$I_{electron}$/A	energy step/eV
200	0.1428	0.073	0.075	0.3∼0.5	200
400	0.1725	0.1151	0.075	1.0	410

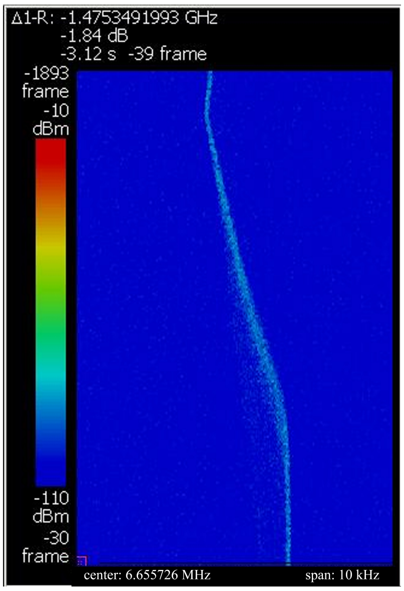

Fig. 4. Schottky signal after 410 eV electron energy step.

The influence of the electron beam intensity on the longitudinal cooling force for $^{12}C^{6+}$ beam was studied experimentally. The cooling force increases with increased electron beam centre density as shown in Fig. 5.

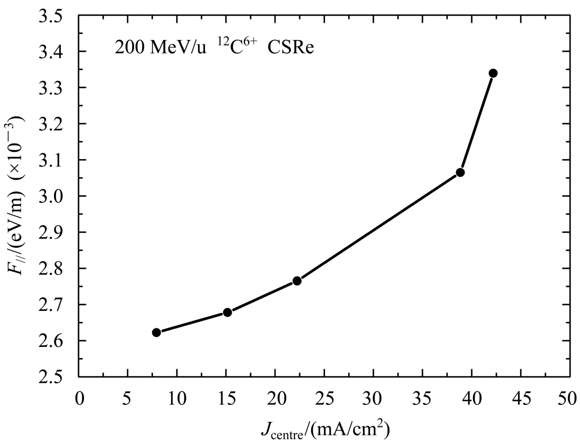

Fig. 5. Longitudinal cooling force measured for $^{12}C^{6+}$ ion as a function of different centre densities of different electron beam profiles.

The dependence of the longitudinal cooling force on the alignment angles between the ion and the electron beam in transverse direction was measured for $^{12}C^{6+}$ ions. The longitudinal cooling force as function of the alignment angle is shown in Fig. 6 and Fig 7. It's obvious that perfect alignment is helpful for obtaining maximum longitudinal cooling force.

Longitudinal cooling forces were obtained for 200 MeV/u $^{12}C^{6+}$ and 400 MeV/u $^{12}C^{6+}$ by the electron energy-step method. The experimental results were in best agreement with the semi-empirical formula. The longitudinal cooling force increased with the increasing electron beam current, and decreased the alignment angle between the ion and electron beams. According to the experimental results, the momentum cooling time of 15 s for 400 MeV/u $^{12}C^{6+}$ was obtained in HIRFL-CSRe.

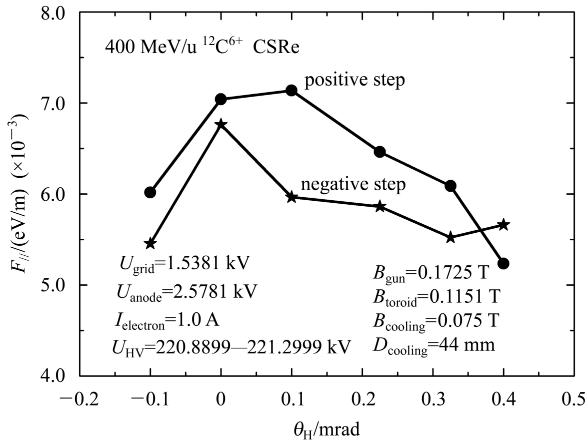

Fig. 6. Longitudinal cooling force for different relative horizontal angles of electron beam.

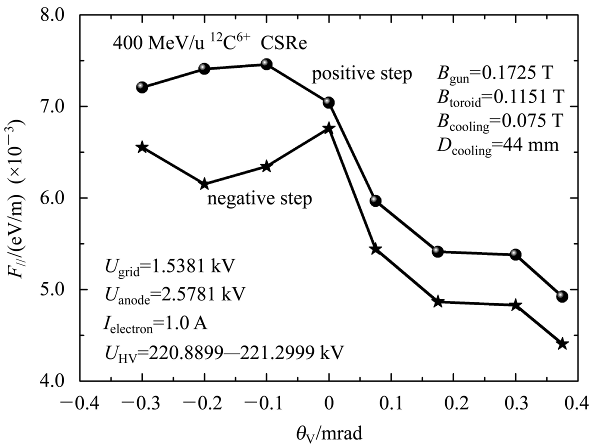

Fig. 7. Longitudinal cooling force for different relative vertical angles of electron beam.

Due to the positions between the ion beam and the electron, the electron density distribution, and the initial electron energy not being perfectly optimized, different results appeared between the negative energy step and the positive energy step.

2.4 Beam lifetime

The lifetime of the heavy ion beam in the storage ring was a complicated problem. It was determined by the scattering due to the molecule and atom of residual gas, the internal gas target, the charge state changing due to ion capture electron and the ionization.

After one pulse ion beam was injected to CSRe, the injection was stopped and CSRe operated in the mode of DC. The lifetime was measured with the help of the DCCT signal. Due to the influence of the kicker and other ramping elements, the ion beam decayed fast at the beginning, after the field of the kicker and other element disappeared completely, the ion beam decayed very slowly. The lifetime of 400 MeV/u $^{12}C^{6+}$ in CSRe is shown in Fig. 8. From the fitting results, the lifetime was over 80 h.

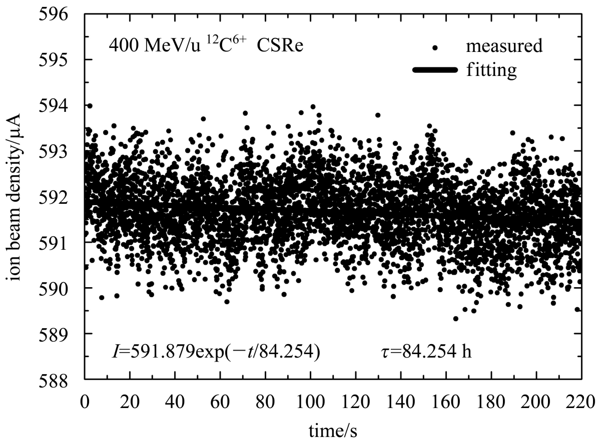

Fig. 8. The ion beam lifetime after electron cooling.

2.5 Intrabeam scattering

The electron beam was turned off after the ion beam was cooled to the equilibrium. The Intrabeam Scattering and the diffusion of residual gas were investigated. All particles suffered from the action of vacuum, this caused the energy loss, and the momentum shift. But IBS happened in certain conditions, it made the momentum spread become bigger (longitudinal blow-up). If the electron beam was switched off after cooling, these two processes happened synchronously, after some time the IBS disappeared, and only the vacuum action still existed. The momentum spread varying with the time is shown in Fig. 9.

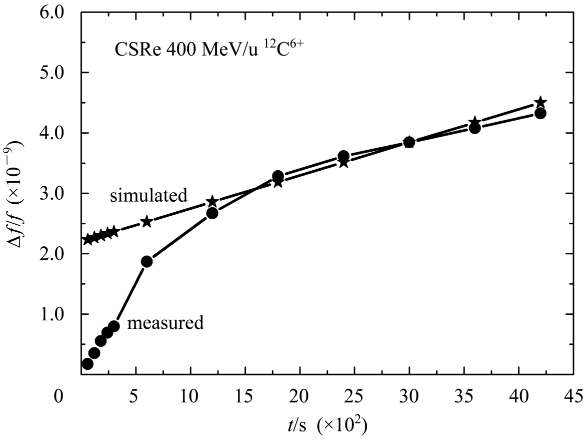

Fig. 9. The central frequency shift due to residual gas of vacuum, the dot and line represent the measured results, the star and line represent the simulated results by the Bethe formula.

At the beginning, the momentum spread increased very fast, it was caused by the IBS, after this the scattering of residual gas was dominated, the slide of change became smaller than at the beginning. The centre frequency shift is shown in Fig. 10. Compared with the simulation results from Bethe formula, the two results were in good agreement.

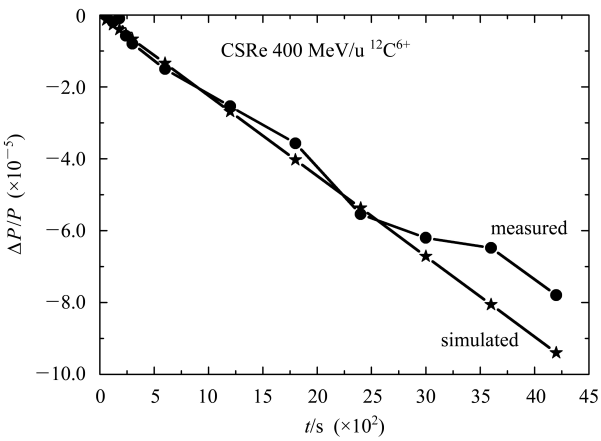

Fig. 10. The momentum spread varies over time after the electron beam was switched off. The dot and line represent the measured results, the star and line represent the simulated results by the Bethe formula.

2.6 Stability of high voltage

From those results after the electron beam was switched off, the stability of high voltage system of CSRe cooler was derived. The data of high voltage (HV) was recorded as one file, the high voltage value was derived from the ion beam revolution frequencies, Fig. 11 shows the results of stability of HV of CSRe cooler, the thin line–electron energy from ion energy, the middle line–signal from divider resistor 1 of HV system, the lower line–signal from divider resistor 2 of HV system, one can find that as the electron beam energy slightly decreased, the ion beam was moved from the initial point to another point with the change of electron energy. From this point of view, the stability of HV system of CSRe cooler should be improved in the future.

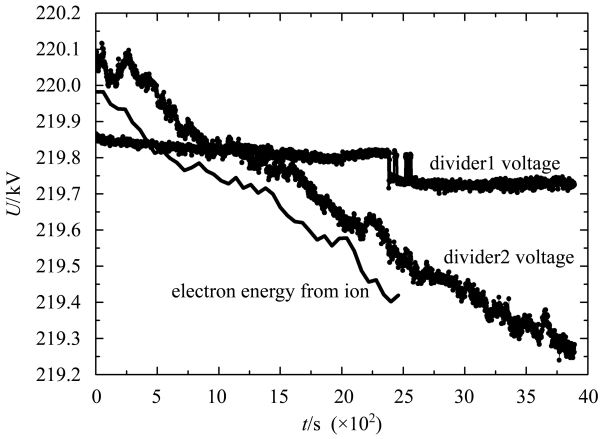

Fig. 11. The stability of CSRe HV system of cooler.

2.7 Beam transverse dimension measurement

Since the transverse profile monitors were not available in CSRe, a movable screen driven by step motor was employed to measure the transverse dimension of the ion beam. The average moving speed was about 1 mm/s, during the screen movement, the ion density signal was recorded by the DCCT in CSRe as shown in Fig. 12. The loss rate of ion information was obtained in this way, and the transverse dimension of the ion beam was derived from this signal. The transverse dimension was about 24 mm before cooling, it was reduced to 1 mm after cooling. The measurement results are shown in Fig. 13.

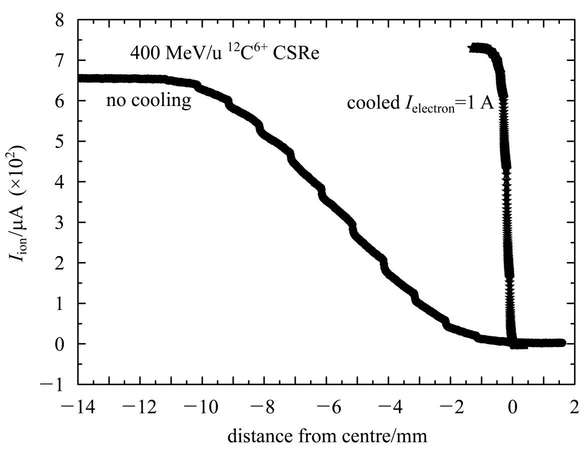

Fig. 12. The DCCT signal when moving the screen. The average moving speed was about 1 mm/s.

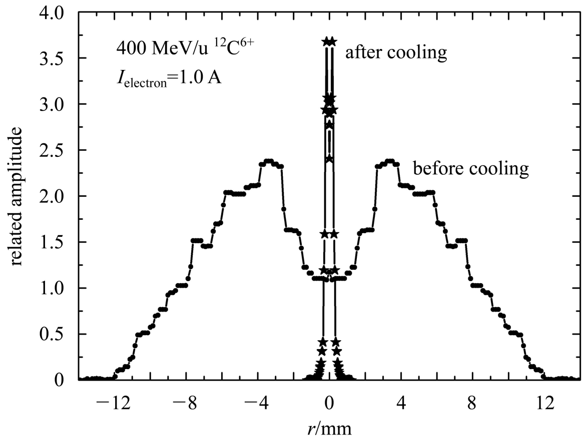

Fig. 13. The transverse ion beam size, the solid line–before cooling, the dot line–after cooling.

From the measured ion beam diameters, the emittance of the ion beam were estimated by $\sigma=\sqrt{\varepsilon\cdot\beta}$, the Betatron function in the position of the screen was about 4 m, and the emittance of ion beam varied from 36 πmm·mrad(3σ) to 0.06 πmm·mrad(3σ) before and after cooling.

2.8 Bunch length measurement

The bunch length was measured with the help of the signal from pick-up electrodes of the beam position monitor after the ion beam was bunched by the RF cavity in CSRe.

The bunch length varying with the average ion beam current is shown in Fig. 14. In the case of lower

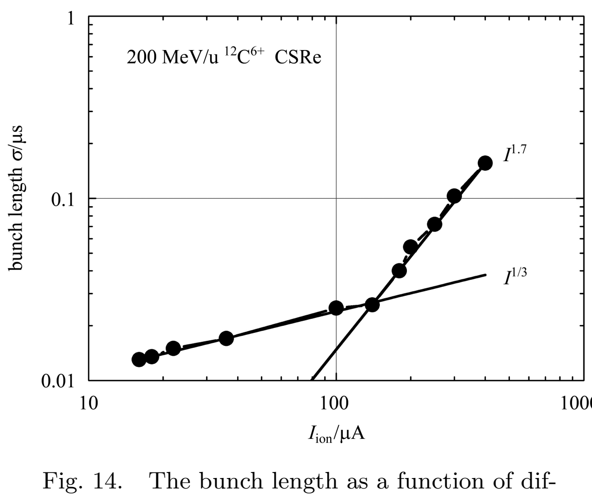

Fig. 14. The bunch length as a function of different average ion beam current.

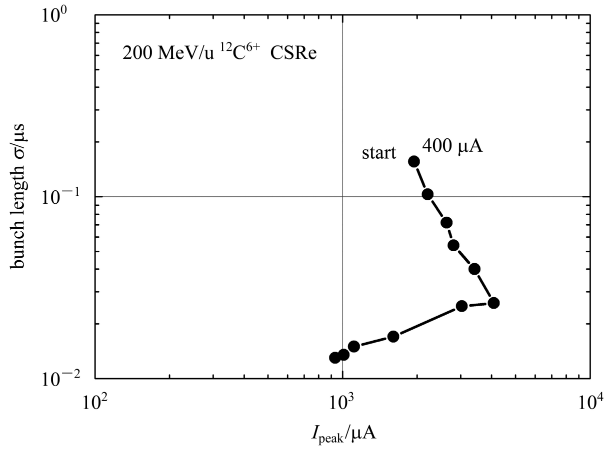

Fig. 15. The bunch length as a function of peak current of the ion beam.The peak current was derived from the average current and bunch length.

ion beam density, the bunch length increased as $I^{1/3}$ with the beam density. It is in agreement with the theoretical calculation that corresponds to the action of space charge which was compensated by the RF voltage, but in the case of higher ion density, the bunch length increased as $I^{1.7}$, it seems that another factor influences the bunch length. If the average ion current was converted to peak density as shown in Fig. 15, it was clear that the peak current achieved to a few mA, and the corresponding Laslett tune shift approached near -0.1. The bunch length decreased quickly in the beginning from start measurement, and the beam peak current increased quickly, after approaching the space charge limitation, the beam lost quickly, and then the bunch length slightly decreased with the ion peak current decreasing.

3 Summary and outlook

The CSRe electron cooler has come to the routine operation for experiments with stored heavy ion beams in HIRFL-CSR. The cooling process of 400 MeV/u $^{12}C^{6+}$ ion beam was studied in CSRe, the main parameters such as momentum spread, transverse ion beam size, and lifetime of stored ion beam were measured. The longitudinal cooling force was measured in the cases of different electron beam profiles, and the different angles between the ion beam and the electron beam. Some initial results of IBS and residual gas scattering were investigated based on the experimental results. The emittance and momentum spread of the ion beam after electron cooling approached the designed value and satisfied the requirements of physics experiments.

References

1 XIA J W et al. High Power Laser & Particle Beams, 2008, **20**(11): 1787 (in Chinese)
2 Antokhin E I, Bocharov V N, Bubley A V et al. NIM A, 2000, **441**: 87
3 Bocharov V N, Bubley A V, Boimelstein Y et al. NIM A, 2004, **532**: 144
4 Behtenev E, Bochanov V N, Bubley A V et al. Commission of Electron Cooler EC-300 for HIRFL-CSR, RuPAC XIX Dubna Russia, 2004. 506–510
5 Behtenev E, Bochanov V N, Bubley A V et al. Commission of Electron Cooler EC-300 for HIRFL-CSR. EPAC 2004 Lucerne Switzerland, 2004. 1419–1421
6 Behtenev E, Bochanov V N, Bubley A V et al. Commission of Electron Cooler EC-300 for HIRFL-CSR. COOL'05, Galena, Illinois, USA 18–23 September 2005. AIP Conference Proceedings, 2006, **821**: 334–340
7 Veremeenko V M, Voskoboynikov R V, Gonchanov A D et al. High Voltage Power Supplies for Ion Beams Electron Coolers. RuPAC 2006, Novosibirsk, Russia, 2006. 97–99
8 YANG X D et al. Commissioning of Electron Cooling in CSRm. COOL'07. Bad Kreuznach, Germany, September, 2007. 59–63 http://accelconf.web.cern.ch/AccelConf/cl07/PAPERS/TUM1I02.PDF
9 Steck M et al. NIM A, 2004, **532**: 357
10 Meshkov I, Sidorin A, Smirnov A et al. Necessary Condition for Beam Ordering. COOL'07. Bad Kreuznach, Germany, September, 2007, 87–90. http://accelconf.web.cern.ch/AccelConf/cl07/PAPERS/TUA1C03.PDF
11 Bosser J Electron Cooling, CAS CERN Accelerator School, Fifth Advanced Accelerator Physics Course, CERN95-06, 1995. 673-730
12 MAO L J, LI G H, LI J et al. http://cool09.impcas.ac.cn/JACoW/papers/thm1mcco03.pdf